

Microporous Polyethylene and Cellulose Composite Separators for Reversible Lithium Electrode in Lithium Rechargeable Batteries

Yuna Hirai,^[a] Rio Ohnishi,^[a] Sou Taminato,*^[a] Daisuke Mori,^[a] Hiroki Eimura,^[b] Kei Ikoma,^[b] Atsushi Sawamoto,^[b] Osamu Yamamoto,*^[a] Yasuo Takeda,^[a] and Nobuyuki Imanishi^[a, c]

The lithium metal anode is the best candidate for high energy density batteries because of its high specific capacity and low negative potential. Rechargeable lithium metal batteries (RLMB) have not yet been commercialized. The key factors that limit the practical use of RLMB are the formation and growth of lithium dendrites during the lithium deposition process and the reaction of the lithium anode with the organic solvent of the electrolyte, quantified by the Columbic efficiency (CE). To suppress the lithium dendrite formation and to improve CE, many approaches such as the formation of a protective layer on

the lithium electrode and the use of additives to the electrolyte have been proposed. In this study, the effect of a thin cellulose film to improve CE of lithium deposition and stripping on the lithium electrode was examined. The cycle performance of a Li/Li symmetrical cell with a cellulose and polyethylene composite separator was examined for a carbonate electrolyte and an ether electrolyte. The improvements of CE were observed for both electrolytes with the cellulose film separator. The improvement could be explained by the good wettability of the cellulose film separator with the electrolyte.

1. Introduction

The energy densities of current lithium-ion secondary batteries (LIBs) are typically between 100 and 200 Wh kg⁻¹ (cell level). However, the electric vehicle (EV) market demands an even higher specific energy of more than 500 Wh kg⁻¹ at the cell level.^[1] Many types of high energy density rechargeable batteries, such as lithium metal,^[2] lithium air,^[3] lithium sulfur,^[3] and solid-state^[4] have been proposed and developed. Lithium-metal batteries are one of the most promising batteries with an energy density of more than 500 Wh kg⁻¹ due to high specific capacity and low potential of the lithium anode.^[2] Lithium-metal rechargeable batteries have been extensively studied after the first report of the lithium intercalation reaction into TiS₂.^[5,6] However, rechargeable lithium metal batteries have not yet been commercialized, except for a short period in the late 1980s,^[7] because of lithium dendrite formation during the

lithium deposition process, which results in short-circuiting of the cell. Many approaches, such as the adoption of a high lithium ion concentration electrolyte,^[8] the addition of LiF into the electrolyte solution,^[9] protection of the lithium electrode with Nafion^{TM[10]} and protein films,^[11,12] and the use of bimetallic three dimensional metal-organic framework-base separators,^[13] and cellulose separators^[14-16] have been employed for many years to suppress lithium dendrite formation and to improve cyclic performance on the lithium electrode. The lithium deposition and stripping performance has been considerably improved.^[17-19] However, further investigation is required for these batteries to be applied in EVs. In particular, improvement for long life stability at high current density and at an acceptable capacity is required.

Here, focus has been made on the effect of a commercialized thin cellulose separator (10 µm thick) for the lithium deposition and stripping processes in the ether based and carbonate based electrolytes. The cellulose separator was introduced by Goodenough and co-workers in 2016,^[15] where a cellulose-based porous membrane of Masked Pack (30 µm thick) was used. A Li/1 M LiCF₃SO₃-0.5 M LiNO₃ in 1,3 dioxolane (DOL)-1,2 dimethoxyethane (DME) (1:1 v/v)/Li cell with the cellulose separator showed no short-circuit for 200 h at 2.4 mA cm⁻² and 2 h polarization, while a cell with a Celgard® 2500 separator (CG) showed a short-circuit for 40 h at 2.4 mA cm⁻² and 2 h polarization. In 2017, Manthiram and co-workers^[20] also reported good cycle performance for a Li/1.85 M LiCF₃SO₃ in DOL-DME (1:1 v/v)/Li cell at 5 mA cm⁻² and 3 h polarization; no short-circuit for 1000 h operation with cellulose-based Kimwipe paper (KW; 50 µm thick) and CG used as a separator. They claimed the excellent lithium electrode performance was due to the polar functional groups acting as a media to facilitate uniform Li-ion distribution on the electrode.

[a] Y. Hirai, R. Ohnishi, S. Taminato, D. Mori, O. Yamamoto, Y. Takeda, N. Imanishi
Graduate School of Engineering, Mie University, Tsu, Mie 514-8507, Japan
E-mail: taminao@chem.mie-u.ac.jp
yamamoto@chem.mie-u.ac.jp

[b] H. Eimura, K. Ikoma, A. Sawamoto
TORAY Industries, Inc., Films & Film Products Research Laboratories, 1-1-1, Sonoyama, Otsu, Shiga 520-8558, Japan

[c] N. Imanishi
Research Center for Integrated Materials and Interfaces for Sustainable Energy, Mie University, Tsu, Mie 514-8507, Japan

Supporting information for this article is available on the WWW under <https://doi.org/10.1002/batt.202400472>

© 2024 The Authors. *Batteries & Supercaps* published by Wiley-VCH GmbH. This is an open access article under the terms of the Creative Commons Attribution License, which permits use, distribution and reproduction in any medium, provided the original work is properly cited.

We have previously reported^[21] excellent cycle performance for a Li/1 M Li(FeO₃)₂N in 1,4 dioxane (DX)-DME (1:2 v/v)/Li cell with KW/CG/KW as a separator at 5 mA cm⁻² for 1 h polarization. The excellent performance of the lithium electrode was explained by the 3 D structure of the Li/KW electrode. The KW separator is effective with an ether based electrolyte but not with a carbonate based electrolyte. In this study, we examined the effect of a thin cellulose separator (CS; Nippon Kodoshi Co. 10 µm thick) on the lithium electrode performance in ether based and carbonate based electrolytes.

2. Results and Discussion

2.1. Cycle Performance of Li/Non Aqueous Electrolyte/Li With CS and ST

A symmetrical Li/1 M LiPF₆ in ethylene carbonate (EC)-diethyl carbonate (DEC) (1:1 v/v)/Li cell with CS was prepared to investigate the performance of CS. Carbonate electrolytes are more commonly used in high voltage lithium-ion batteries due to their high boiling points, low cost, and wide electrochemical windows.^[22] However, the plating and stripping efficiency of lithium metal in an electrolyte with a carbonate solvent has been reported to be poor with a coulombic efficiency (CE) as low as 80%.^[23] Figure 1(a) shows the galvanostatic cycle performance of the Li/1 M LiPF₆ in EC-DEC(1:1 v/v)/Li cell with CS at 1 mA cm⁻² for 1 h polarization and 10 min. rest and at

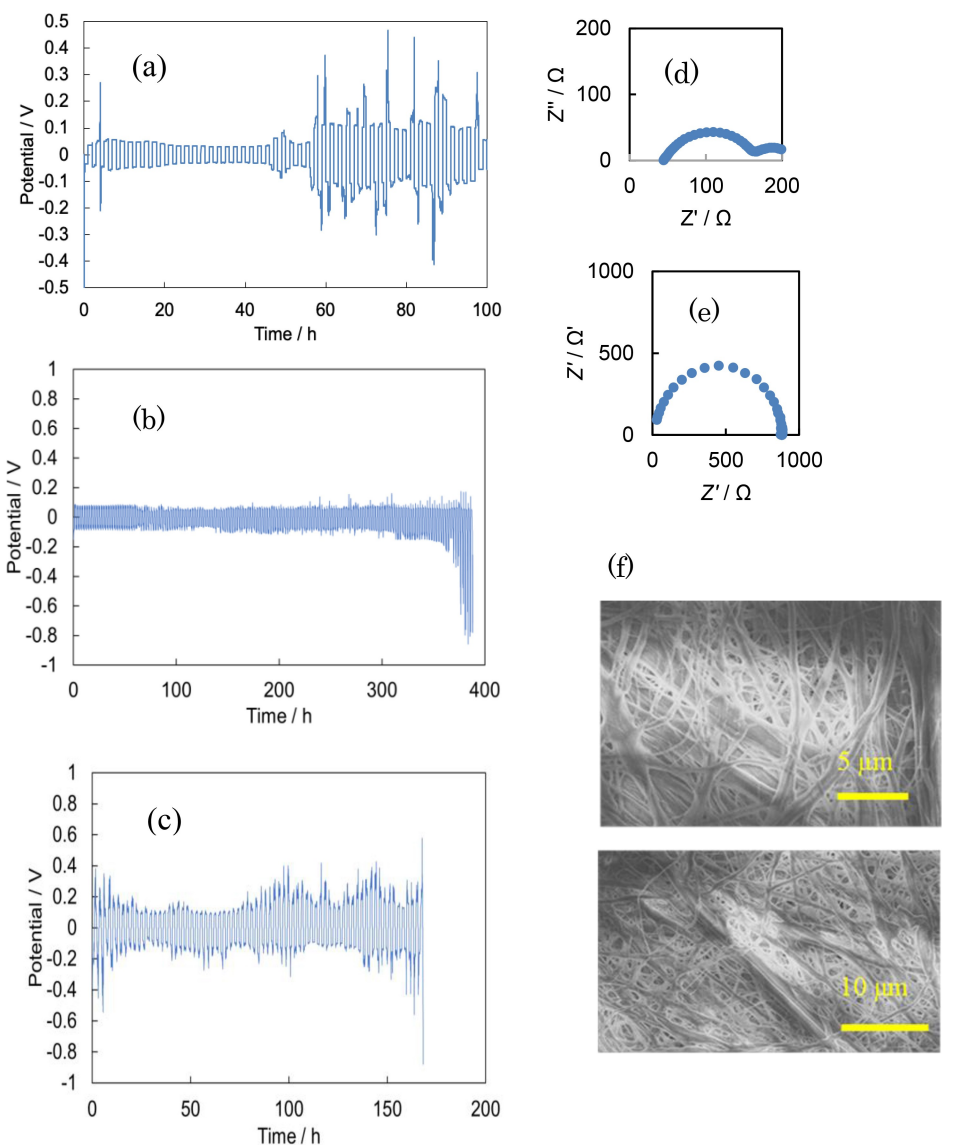


Figure 1. Cycle performance of (a) Li/1 M LiPF₆ in EC-DEC (1:1 v/v), 50 µL/Li with CS at 1.0 mA cm⁻², (b) Li/1 M LiPF₆ in EC-DEC (1:1 v/v, 50 µL)/Li with ST at 1 mA cm⁻² and (c) 5 mA cm⁻² for 1 h polarization at 25 °C. Cell impedance profiles of Li/1 M LiPF₆ in EC-DEC (1:1 v/v)/Li with CS (d) before and (e) after cycling at 1.0 mA cm⁻². (f) SEM images of CS.

25 °C. The CS has large pores as shown in Figure 1(f). Park et al.^[24] reported that a Li/1 M LiPF₆ in EC-dimethyl carbonate (DMC)-ethyl methyl carbonate (EMC) (1:1:1 v/v)/Li cell with a 1 mm thick Teflon separator was short-circuited after 11 min polarization at 1.0 mA cm⁻². In contrast, the cell with the CS separator showed no short-circuit for around 60 h, and the cell voltage increased after 25 cycles at 1 mA cm⁻² and 1 mAh cm⁻². The increase in the cell potential may be due to the formation of reaction products from the lithium electrode and electrolyte. The cell impedances before and after polarization are shown in Figure 1(d) and (e); the initial cell resistance of 210 Ω was increased to 870 Ω. The cycle performance of a Li/Li cell with the same electrolyte and a microporous polyethylene separator (ST) (SETELA™, Toray; 10 μm thick and 20–100 nm pore size) is shown in Figure 1(b) at 1 mA cm⁻² for 1 h polarization and Figure 1(c) at 5 mA cm⁻² for 1 h polarization. The cell voltages were increased after around 350 h at 1.0 mA cm⁻² and after 170 h at 5.0 mA cm⁻² with no short-circuit observed. Choudhury and Archer^[25] reported the cycle performance of Li/1 M LiPF₆ in EC-DMC/Li with a Celgard® separator (CG) at 1.0–4.0 mA cm⁻² for 4 h polarization. The cell potentials also increased after around 800 h at 1.0 mA cm⁻² and after 80 h at 4.0 mA cm⁻². They also claimed that the increases in voltage are an indication of electrolyte degradation by side reactions. Zhao et al.^[9] also reported the cycle performance of a Li/LiPF₆ in EC-DEC/ /Li cell with CG at 1.0–5.0 mA cm⁻² for 1 h polarization, where the cell could be operated for around 280 h at 1.0 mA cm⁻² and 50 h at 5.0 mA cm⁻² before cell voltage fluctuation. The cell voltage fluctuation was confirmed to be due to drying up of the organic electrolyte and dendrite-induced short-circuit. The period until fluctuation of the cell voltage was increased by an increase in the amount of electrolyte.

Figure 2 shows the galvanostatic cycle performance of a symmetrical Li/1 M LiPF₆ in EC-DEC (1:1 v/v, 50 μL)/Li cell with a triple composite separator of CS/ST/CS at (a) 1.0 mA cm⁻² and (b) 5.0 mA cm⁻² for 1 h polarization and 10 min rest and at 25 °C. The Li/Li cell potentials for the cell with the ST separator fluctuated after 350 h at 1.0 mA cm⁻² and after 170 h at 5 mA cm⁻². In contrast, the cycle performance for the Li/Li cell with the CS/ST/CS triple separator was considerably improved. The cell with the CS/ST/CS triple separator could be operated for more than 750 h at 1 mA cm⁻² and for 550 h at 5.0 mA cm⁻²

The Coulombic efficiency (CE) for lithium deposition and stripping on the lithium metal electrode is an important property of the lithium electrode for lithium metal batteries. If we define 50% capacity retention after 1000 cycles, then the CE would have to be as high as 99.93%.^[26] Choudhury and Archer^[25] examined the CE for Li/1 M LiPF₆ in EC-DMC/ stainless steel (SS). The estimated CE was close to 80%, whereas they observed a high CE of 99% for Li/1 M LiPF₆ in EC-DMC/LiFePO₄ at 0.5 mA cm⁻². Imanishi and co-workers^[27] proposed a new method to determine the CE for lithium deposition and stripping on lithium metal from the loss of electrolyte using a Li/electrolyte/Li cell with a limited amount of electrolyte. The CE was estimated using the following equation:

$$CE = 1 - C_1/C_2 \quad (1)$$

where C₁ is the electrochemical capacity of the electrolyte solvent for reaction with lithium and C₂ is the capacity passed through the cell. The CE of 98.4% for the Li/1 M LiPF₆ in EC-DEC (1:1 v/v)/Li cell with the ST separator at 5 mA cm⁻² was enhanced to 99.5% for the cell with the CS/ST/CS triple separator.

The ether based electrolytes have been extensively studied for lithium metal electrodes because of their high solubility for lithium salts and wide potential window. The electrolyte of 4 M LiFSI in DME could be cycled at 10 mA cm⁻² and 5 mAh cm⁻² for 600 h,^[28] however, an electrolyte with a high content of LiFSI is quite expensive and has a high viscosity. The Li/1 M LiFSI in 1,4 dioxane (DX)-DME (1:2 v/v)/Li with polyethylene separator cell showed excellent cycle performance at 5 mA cm⁻² and 8.5 mAh cm⁻² for 110 h without fluctuation of the cell potential.^[29] We have previously reported^[14] that a Li/1 M LiPF₆ in DX-DME (1:2 v/v)/Li cell with a KW separator showed excellent cycle performance at 5 mA cm⁻² and 5 mAh cm⁻² with no fluctuation of the potential for 1100 h. The excellent cycle performance was explained by the formation of a 3D lithium electrode inside the KW separator (ca. 50 μm thick KW). In this study, we have examined the lithium deposition and stripping cyclic performance in 1, 2-diethoxyethane (DEE) with the thin cellulose separator (ca. 10 μm thick). DEE has a higher boiling point than DME. Figure 3(a) shows the cycle performance of a Li/1 M LiTFSI in DEE (50 μL)/Li cell with ST at 1.0 mA cm⁻² and

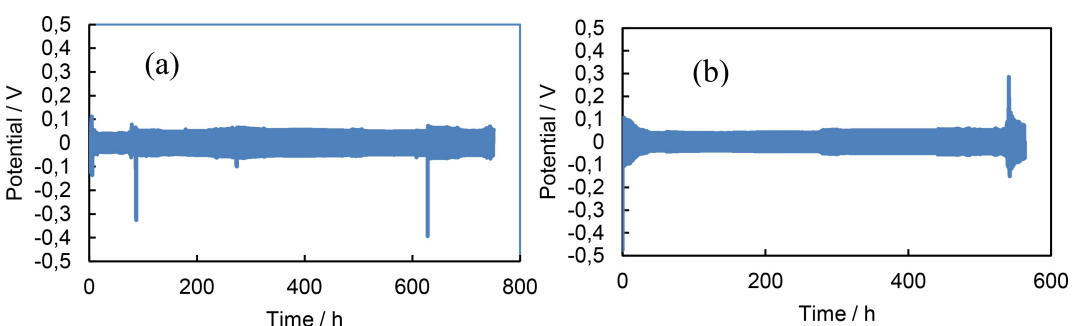


Figure 2. Cycle performance of Li/1 M LiPF₆ in EC-DEC (1:1 v/v, 50 μL)/Li with a CS/ST/CS triple separator (a) at 1.0 mA cm⁻² and (b) at 5.0 mA cm⁻² and at 25 °C.

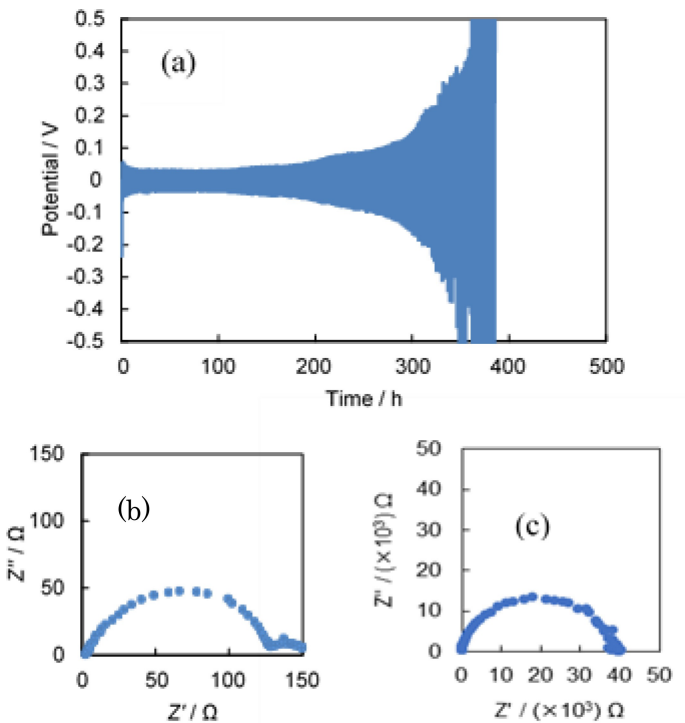


Figure 3. (a) Cycle performance of Li/1 M Li TFSI in DEE/Li (50 μ L) with ST at 1 mA cm^{-2} for 1 h polarization and at 25 $^\circ\text{C}$ and cell impedance profiles (b) before and (c) after cycling.

1 mAh cm^{-2} and 25 $^\circ\text{C}$. The cell with the ST separator showed an increase in the cell potential after 200 h cycling. The potential increase could be explained by an increase in the cell resistance due to electrolyte decomposition. The initial cell impedance of around 150 Ω increased to $4 \times 10^4 \Omega$ after cycling, as shown in Figures 3(b) and (c). The estimated CE of lithium deposition and stripping on lithium was 96.8%. Figure 4 shows the cycle performance of a Li/1 M LiTFSI in DEE(50 μ L)/Li cell with the CS/ST/CS triple separator at 1 mA cm^{-2} for 1 h polarization and 5 mA cm^{-2} for 1 h polarization. The cell with the CS/ST/CS triple separator was cycled for 625 h at 5 mA cm^{-2} . The CE at 5 mA cm^{-2} was estimated to be 99.6% using the amount of

charged electrolyte (50 μ L). Table 1 summarizes the CE for the lithium deposition and stripping of the Li/1 M LiPF₆ in EC-DEC/Li cells with ST and CE/ST/CE separators and the Li/1 M LiTFSI in DEE/Li cells with ST and CE/ST/CE separators, where CE was calculated based on one electron reaction of lithium and electrolytes. High CEs of 99.5% for Li/1 M LiPF₆ in EC-DEC (1:1 v/v) and 99.6% for Li/1 M LiTFSI in DEE/Li with the CS/ST/CS triple separator at 5 mA cm^{-2} and 5 mAh cm^{-2} were observed. Such a high CE at a high current density is attractive for long-life rechargeable lithium batteries for EV applications.

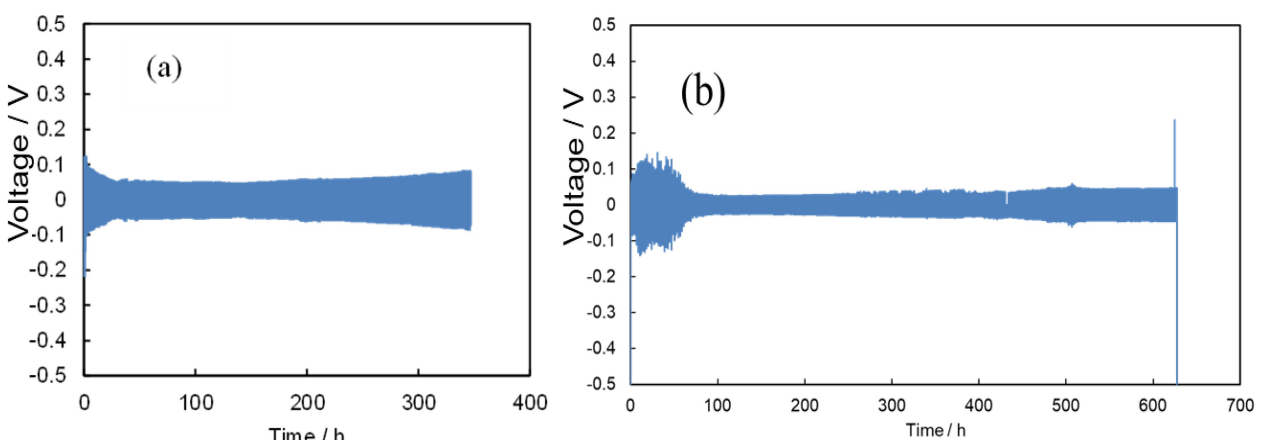


Figure 4. (a) Cycle performance of Li/1 M LiTFSI in DEE (50 μ L)/Li with CS/ST/CS at (a) 1 mA cm^{-2} for 1 h at 25 $^\circ\text{C}$ and (b) 5 mA cm^{-2} for 1 h at 25 $^\circ\text{C}$.

Table 1. CEs of lithium deposition and stripping for Li/1 M LiPF₆ in EC-DEC/Li and Li/1 M LiTFSI in DEE/Li with CS, ST and CS/ST/CS separators.

Separator	Electrolyte	Current density (mA cm ⁻²)	CE (%)
CS	1 M LiPF ₆ in EC-DEC	1.0	80
ST	1 M LiPF ₆ in EC-DEC	1.0	96.5
ST	1 M LiPF ₆ in EC-DEC	5.0	98.4
CS/ST/CS	1 M LiPF ₆ in EC-DEC	1.0	>98.1
CS/ST/CS	1 M LiPF ₆ in EC-DEC	5.0	99.5
ST	1 M LiTFSI in DEE	1.0	96.8
CS/ST/CS	1 M LiTFSI in DEE	1.0	>96.8
CS/ST/CS	1 M LiTFSI in DEE	5.0	99.6

2.2. Lithium-Ion Transport Numbers and Electrochemical Stability of 1 M LiPF₆ in EC-DEC and 1 M LiTFSI in DEE

Lithium-ion transport numbers of 1 M LiPF₆ in EC-DEC (1:1 v/v) and 1 M LiTFSI in DEE were measured using the method reported by Evans et al.^[30] Figure S1 shows the current decay curve upon application of a 10 mV bias and the impedance

profile changes before and after polarization for the Li/1 M LiPF₆ in EC-DEC (1:1 v/v)/Li and Li/1 M LiTFSI in DEE/Li cells with ST and CS/ST/CS at 25 °C. The lithium-ion transport numbers, T_{Li+} , were calculated by the following equation;

$$T_{Li+} = I^s(\Delta V - I^o R_i^o) / I^o (\Delta V - I^s R_i^s) \quad (2)$$

where I^s and I^o are the initial and steady-state currents, respectively, R_i^o and R_i^s are the initial and steady-state resistance of the passivating layers, respectively, and ΔV is the potential applied across the cell. Table 2 summarizes the lithium-ion transport numbers estimated for Li/1 M LiPF₆ in EC-DEC (1:1 v/v)/Li with ST and CS/ST/CS and Li/1 M LiTFSI in DEE/Li with ST and CS/ST/CS. The lithium-ion transport numbers of 1 M LiPF₆ in EC-DEC and 1 M LiTFSI in DEE with the CS/ST/CS composite separator are slightly higher than those with ST. The lithium-ion transport number of 0.22 for 1 M LiPF₆ in EC-DEC with ST is comparable to that of 0.24–0.28 reported by Zugmann.^[31] The high lithium-ion transport number of 0.65 was observed in 1 M LiTFSI in DEE with CS/ST/CS, which is slightly higher than that of 0.59 in 1 M LiTFSI in DEE with ST.

The electrochemical stability of 1 M LiPF₆ in EC-DEC (1:1 v/v) and 1 M LiTFSI in DEE with ST and CS/ST/CS was measured using linear scanning voltammetry (LSV). Figure 5 shows the results for the Li/1 M LiPF₆ in EC-DEC (1:1 v/v)/stainless steel (SS) and Li/1 M LiTFSI in DEE/SS with ST and CS/ST/CS cells within a voltage range of 1.5–5 V at a scan rate of 5 mV s⁻¹. The both electrolytes with ST and CS/ST/CS are stable up to 4.2 V.

Table 2. Lithium-ion transport numbers of 1 M LiPF₆ in EC-DEC (1:1 v/v) and 1 M LiTFSI in DEE with ST and CS/ST/CS at 25 °C.

Electrolyte	Separator	Lithium-ion transport number
1 M LiPF ₆ in EC-DEC (1:1 v/v)	ST	0.22
1 M LiPF ₆ in EC-DEC (1:1 v/v)	CS/ST/CS	0.23
1 M LiTFSI in DEE	ST	0.59
1 M LiTFSI in DEE	CS/ST/CS	0.65

2.3. Cell Resistances of Li/1 M LiPF₆ in EC-DEC (1:1 V/V)/Li And Li/1 M LiTFSI in DEE/Li with ST and CS/ST/CS

The interface of the Li/non-aqueous electrolyte/Li cell shows a high resistance due to the formation of the solid electrolyte interlayer (SEI).^[32] The effect of the CS separator for the interface resistance was examined. Figure 6 shows the cell impedance profiles as a function of the storage period for Li/1 M LiPF₆ in EC-DEC (1:1 v/v)/Li with ST and CS/ST/CS and Li/1 M LiTFSI in

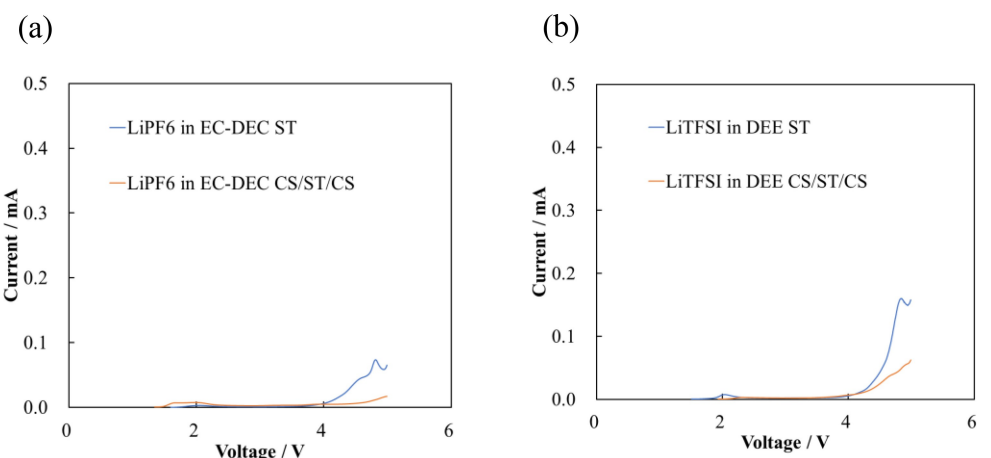


Figure 5. Curves of LSV for (a) Li/1 M LiPF₆ in EC-DEC (1:1 v/v)/SS with ST and CS/ST/CS and (b) Li/1 M LiTFSI in DEE/SS with ST and CS/ST/CS

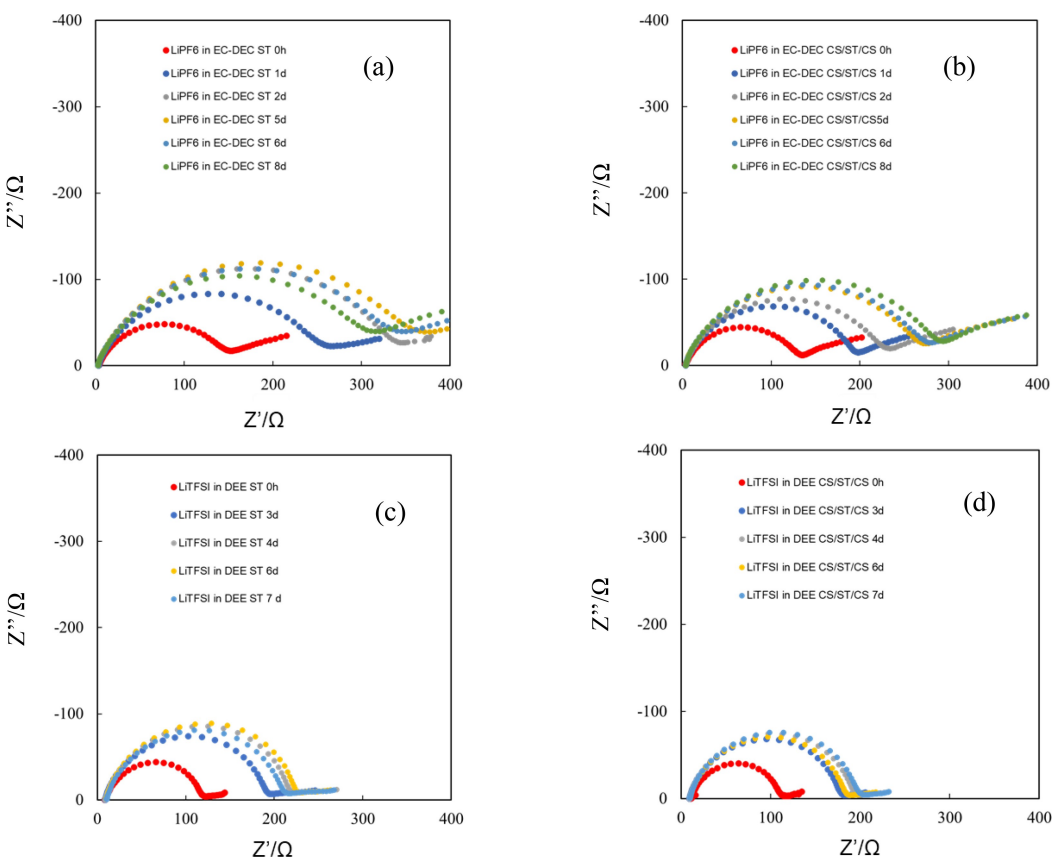


Figure 6. Cell impedance profiles as a function of storage period of (a) Li/1 M LiPF₆ in EC-DEC (1:1 v/v)/Li with ST, (b) Li/1 M LiPF₆-EC-DEC (1:1 v/v)/CS/ST/CS/Li, (c) 1 M LiTFSI in DEE/Li with ST and (d) 1 M LiTFSI in DEE/Li with CS/ST/CS at 25 °C.

DEE/Li with ST and CS/ST/CS. The initial cell resistance of 150 Ω increased to 373 Ω after 5 days for Li/1 M LiPF₆ in EC-DEC (1:1 v/v)/Li with ST. While, that after 8 day for the cell resistance with CS/ST/CS was 306 Ω. Similar interface resistance suppression by the CS separator was observed also for Li/1 M LiTFSI in DEE/Li. The interface resistance of 227 Ω after 6 days for Li/1 M LiTFSI in DEE/Li with ST was decreased to 207 Ω after 6 days for the cell with CS/ST/CS.

2.4. Electrolyte Wettability of the Separators and XPS Analysis of the Lithium Surface

The electrolyte wettability of a separator is an important factor for the lithium deposition and stripping processes.^[20,33–36] To estimate the wettability, the contact angle was measured by dropping electrolytes of 1 M LiPF₆ in EC-DEC (1:1 v/v) and 1 M LiTFSI in DEE onto the ST and CS separators. Figure 7 shows the contact angle test results. The contact angles of 1 M LiPF₆ in EC-DEC (1:1 v/v) on ST and CS were 18.0° and 10.6°, respectively, and those of 1 M LiTFSI in DEE (1:1 v/v) on ST and CS 18.3° and 4.2°, respectively. The CS separator has a low contact angle for the both electrolytes, i.e., the CS separator improves electrolyte wetting.

To understand the effect of the CS/ST/CS separator, the surfaces of lithium electrode contacted with the electrolytes

were analyzed by an X-ray photoelectron spectroscopy (XPS). Figure S2 and S3 shows the Li 1s, C 1s and O 1s XPS spectra of Li surface contacted with 1 M LiPF₆ in DEC-DEC (1:1 v/v) and 1 M LiTFSI in DEE for one week. There are LiOH, Li₂CO₃, and Li₂O on the lithium surface. No clear difference in the XPS spectra between lithium surface with ST and composite of CS/ST/CS was observed in the both electrolytes. The SEI films formed on lithium surface may be similar chemical composition for the cell with ST and CS/ST/CS.

2.5. Full Cell Performance

To verify the function of the CS/ST/CS composite separator, the electrochemical performance of Li/1 M LiPF₆ in EC-DEC/LiNi_{0.5}Mn_{0.3}Co_{0.2}O₂ (NMC) and Li/1 M LiTFSI in DEE/NMC with ST and CS/ST/CS were tested. Figure 8(a) and (b) show the cycle performance at 1.0 mA cm⁻² and 25 °C of Li/1 M LiPF₆ in EC-DEC(1:1 v/v)/ NMC with ST and CS/ST/CS, respectively, where the masses of NMC and Li were 9.5 mg (1.47 mAh at 0.2 C) and 12 mg (46.6 mAh), respectively. The charge and discharge cut-off voltages for cycling were 4.2 and 2.5 V, respectively. Figure 8(c) and (d) show the cycling performance of Li/1 M LiTFSI in DEE/NMC with ST and CS/ST/CS at 1.0 mA cm⁻², respectively. As shown in Figure 8(e) and (f), the cells with the composite separator of CS/ST/CS exhibited better capacity

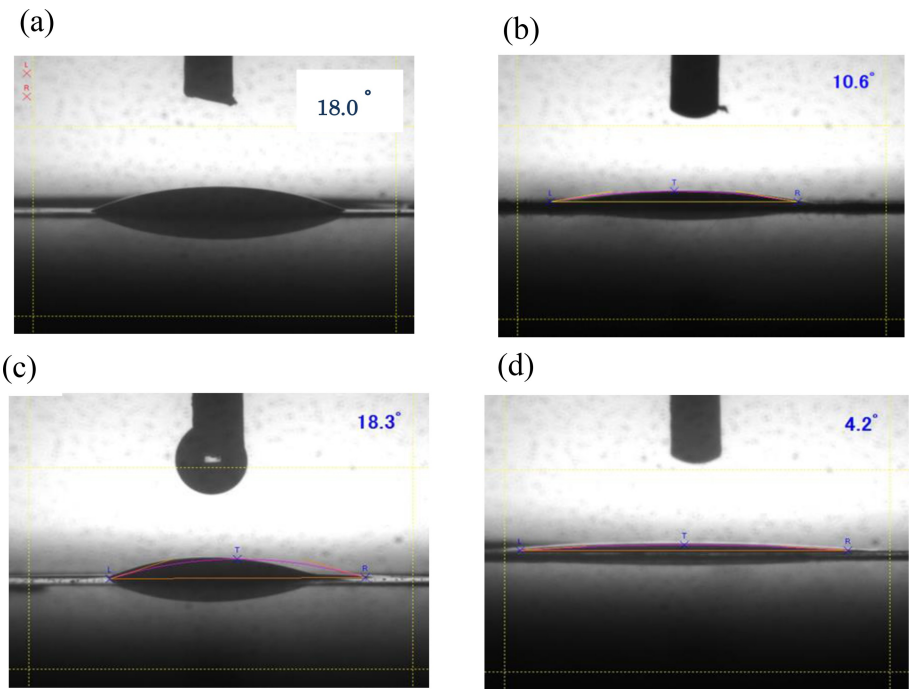


Figure 7. Contact angle images of 1 M LiPF₆ in EC-DEC (1:1 v/v) on (a) ST and (b) CS, and 1 M LiTFSI in DEE on (c) ST and (d) CS.

retention rates compared with those of the cells with ST. The Li/1 M LiTFSI in DEE/NMC cell showed no discharge capacity decrease for 100 cycles at 1.0 mA cm⁻², which present a specific capacity of 124 mAh g⁻¹ at 1.0 mA cm⁻² (0.85 C). The excellent cycle performance of the cell with CS/ST/CS is due to the much higher CE than that with ST. Figures 8(a) and (b) show the rate performance of Li/1 M LiPF₆ in EC-DEC (1:1 v/v)/NMC and Li/1 M LiTFSI in DEE/NMC cells with ST and CS/ST/CS, respectively. Both cells show no significant difference of the rate performance with ST and CS/ST/CS.

3. Conclusions

The lithium deposition and stripping cyclic processes in Li/1 M LiPF₆ in EC-DEC (1:1 v/v)/Li and Li/1 M LiTFSI in DEE/Li with a conventional fine pore polyethylene separator of ST and a ST and a thin cellulose separator of CS composite were showed an increase of the cell potential at a limited number of cycles. The potential increase could be related to the electrochemical decomposition of the electrolyte solvent. The CE for lithium deposition and stripping on a lithium electrode in 1 M LiPF₆ in EC-DEC with ST at 1.0 mA cm⁻² was estimated to be 96.5%. Similar results were obtained for an ether-based electrolyte of 1 M LiTFSI in DEE with ST, where the CE was 96.8%. The CE was improved through the use of a composite separator consisting of CS/ST/CS. The CEs for lithium deposition and stripping with Li/1 M LiPF₆ in EC-DEC/Li and Li/1 M LiTFSI in DEE/Li with CS/ST/CS at 5 mA cm⁻² were estimated to be more than 99.4%. Such a high CE is attractive for rechargeable lithium metal batteries. The contact angle measurement of the electrolyte on the CS separator indicated good wettability of the CS separator with

both electrolytes. The lithium deposition and stripping performance of the cell with the composite separator of CS/ST/CS could be explained by good wettability of the separator with the electrolyte.

Experimental Section

Materials: 10 µm thick cellulose separators (CS; Cellulion®) were obtained from Nippon Kodoshi Co. Japan. The porosity is 60% and the density 0.60 g cm⁻³. 20 µm thick microporous polyethylene separators (ST, SETELA™ 20–100 nm pore size) were obtained from Toray Co., Japan. EC, DEC, and DME were purchased from Kishida Chemical Japan. These solvents were dehydrated using a molecular sieve (3 Å, Kanto Chemical, Japan). Lithium battery grade LiTFSI was obtained from Central Glass Co., Japan.

Electrochemical tests and contact angle measurements: The lithium deposition and stripping cycle performance was measured using 2032-type coin cells. 200 µm thick and 12 cm diameter lithium metal sheets (Honjo Metal, Japan) were used as electrodes. The Li/1 M LiPF₆ in EC-DEC (1:1 v/v)/LiNi_{0.5}Mn_{0.3}Co_{0.2}O₂ (NMC) and Li/1 M LiPF₆ in DEE/ (NMC) full cells with ST and CS/ST/CS were tested in a 2032-type coin cell. NMC was purchased from MTI Co. USA. The electrochemical performance of the cells was measured using a battery cycler (BTS 2004H, Nagano, Japan). The cell impedance was measured using an impedance spectrometer (Solartron 1260). To investigate the wettability of the separators with the electrolytes, the separator/electrolyte contact angle was measured using an optical contact angle measuring system (DMS-400, Kyowa Interface Science, Japan). The surface chemistry of Li was investigated by a XPS/PHI Quantera spectrometer (Ulvac-Phi). The washed Li electrodes were dried and transferred into XPS chamber using an in-house build transfer holder. Scanning electron microscopy (SEM; Hitachi S4800) was used to observe the surface of cellulose separator.

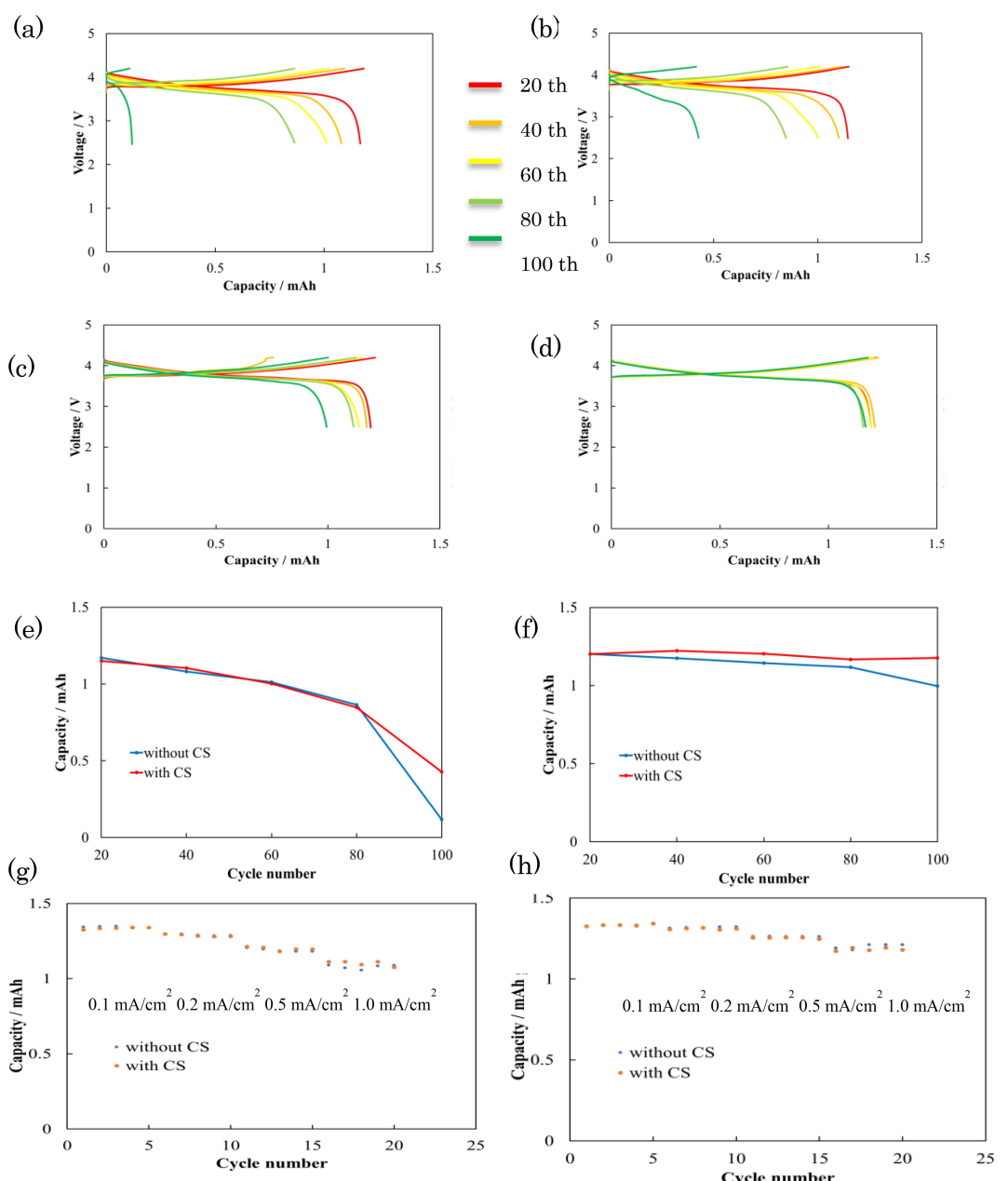


Figure 8. Charge and discharge voltage profiles of Li/1 M LiPF₆ in EC-DEC (1:1 v/v)/NMC with (a) ST and (b) CS/ST/CS at 1.0 mAh cm⁻² and Li 1 M LiTFSI in DEE with (c) ST and (d) CS/ST/CS at 25 °C. Capacity retention with cycle number of (e) Li/1 M LiPF₆ in EC-DEC (1:1 v/v) with ST and CS/ST/CS and (f) Li/1 M LiTFSI in DEE/NMC with ST and CS/ST/CS at 1.0 mAh cm⁻² and at 25 °C. Rate performances of (g) Li/1 M LiPF₆ in EC-DEC (1:1 v/v) and (h) Li/1 M LiTFSI in DEE/NMC with CS and CS/ST/CS at 25 °C.

Acknowledgements

The authors are grateful to Mr. K. Ogawa of Nippon Kodoshi Co. for supply of the cellulose separator material (Cellulion®) and discussion on the properties of the separator.

Conflict of Interests

The authors declare no conflicting interest regarding the content of this article.

Data Availability Statement

The data that support the findings of this study are available on request from the corresponding author. The data are not publicly available due to privacy or ethical restrictions.

Keywords: Cellulose · Contact angle · Cycle performance · Energy conversion · Lithium · Lithium dendrite

- [1] R. Van Noorden, *Nature* **2014**, *507*, 26–28.

- [2] J. Liu, Z. Bao, Y. Cui, E. J. Dufek, J. B. Goodenough, P. Khalifah, Q. Li, B. Y. Liaw, P. Liu, A. Manthiram, Y. S. Meng, V. R. Subramanian, M. F. Toney, V. V. Viswanathan, M. S. Whittingham, J. Xiao, W. Xu, J. Yang, X. Q. Yang, J. G. Zhang, *Nat. Energy* **2019**, *4*, 180–186.
- [3] P. G. Bruce, S. A. Freunberger, L. J. Hardwick, J. M. Tarascon, *Nat. Mater.* **2012**, *11*, 19–29.
- [4] Y. Kato, S. Hori, T. Saito, K. Suzuki, M. Hirayama, A. Mitsui, M. Yomemura, H. Iba, R. Kanno, *Nat. Energy* **2016**, *1*, 1603–1609.
- [5] M. S. Whittingham, *J. Electrochem. Soc.* **1976**, *123*, 315–320.
- [6] M. S. Whittingham, *Solid State Chem.* **1978**, *12*, 41–99.
- [7] Y. Takeda, O. Yamamoto, N. Imanishi, *Electrochim. Acta* **2016**, *84*, 210–218.
- [8] X. Fan, L. Chen, X. Li, T. Deng, S. Hou, J. Chen, J. Zheng, F. Wang, J. Jiang, K. Xu, C. Wang, *Chem.* **2018**, *4*, 174–185.
- [9] J. Zhao, L. Liao, F. Shi, T. Lei, G. Chen, A. Pei, J. Sun, K. Yan, G. Zhou, J. Xie, C. Liu, Y. Li, Z. Liang, Z. Bao, Y. Cui, *J. Am. Chem. Soc.* **2017**, *139*, 11550–11558.
- [10] J. Song, H. Lee, M. J. Choo, J. K. Park, H. T. Kim, *Sci. Rep.* **2015**, *5*, 14458.
- [11] M. Hu, Q. Yang, K. Chen, C. Li, *Energy Technol.* **2023**, *11*, 2300002.
- [12] H. Wu, Q. Wu, F. Chu, J. Hu, Y. Cui, C. Yin, C. Li, *J. Power Sources* **2019**, *419*, 92–81.
- [13] R. Razaq, M. M. U. Din, D. R. Smabren, V. Eyupoglu, S. Janakiran, T. O. Sunde, N. Allahgoli, D. Rettenwander, L. Deng, *Adv. Energy Mater.* **2024**, *14*, 2302897.
- [14] H. Wu, Z. Yao, Q. Wu, S. Fan, C. Yin, C. Li, *J. Mater. Chem. A* **2019**, *7*, 22257–22264.
- [15] B. C. Yu, K. Park, J. H. Jang, J. B. Goodenough, *ACS Energy Lett.* **2016**, *1*, 633–637.
- [16] H. Wu, J. Wang, Y. Zhao, X. Zhang, L. Xu, H. Liu, Y. Cui, C. Li, *Sustainable Energy Fuel* **2019**, *3*, 2642–2656.
- [17] N. Imanishi, T. Zhang, D. Mori, S. Taminato, Y. Takeda, O. Yamamoto, *J. Energy Power Tech.* **2021**, *3*(2).
- [18] B. Song, L. Su, X. Liu, W. Gao, T. Wang, Y. Ma, Y. Zhang, X. B. Cheng, J. He, Y. Wu, *Electron* **2023**, *1*, e13.
- [19] D. Chen, Y. Liu, C. Feng, Y. He, S. Zhou, B. Yuan, Y. Dong, H. Xie, G. Zheng, H. Han, W. He, *Electron* **2023**, *1*, e1.
- [20] C. H. Chang, S. H. Chung, A. Manthiram, *Adv. Sustainable Syst.* **2017**, *1*, 1600034.
- [21] T. Hasegawa, F. Bai, D. Mori, S. Taminato, Y. Takeda, O. Yamamoto, H. Izumi, H. Minami, N. Imanishi, *ChemElectroChem.* **2023**, *10*, 202201043.
- [22] K. Xu, *Chem. Rev.* **2014**, *114*, 11503–11618.
- [23] F. Ding, W. Xu, G. L. Graff, J. Zhang, M. L. Sushiko, X. Chen, Y. Shao, M. H. Engelhard, Z. Nie, J. Xiao, X. Liu, P. V. Sushiko, J. Liu, J. G. Zhang, *J. Am. Chem. Soc.* **2013**, *134*, 4450–4456.
- [24] H. E. Park, C. H. Hong, W. Y. Yoon, *J. Power Sources* **2008**, *178*, 765–768.
- [25] S. Choudhury, L. A. Archer, *Adv. Electron. Mater.* **2016**, *2*, 1500246.
- [26] J. Xiao, Q. Li, Y. Bi, M. Cai, B. Dunn, T. Glossmann, J. Liu, T. Osaka, R. Sugiyra, B. Wu, J. Yang, J. G. Zhang, M. S. Whittingham, *Nat. Energy* **2020**, *5*, 561–568.
- [27] T. Hasegawa, D. Mori, S. Taminato, Y. Takeda, O. Yamamoto, N. Imanishi, *ChemElectroChem.* **2023**, *10*, 202300097.
- [28] H. Qian, W. H. Henderson, W. Xu, P. Bhattacharya, M. Enehard, O. Borodin, J. G. Zhang, *Nat. Comm.* **2015**, *6*, 6362–6371.
- [29] R. Miao, J. Yang, Z. Xu, J. Wang, Y. Nuli, L. Sun, *Sci. Rep.* **2016**, *6*, 21771–21780.
- [30] J. Evans, C. A. Vincent, P. G. Bruce, *Polymer* **1987**, *28*, 2324–2328.
- [31] S. Zugmann, M. Fleischmann, M. Amereller, R. M. Gschwind, H. D. Wiemhofer, H. J. Gures, *Electrochim. Acta* **2011**, *56*, 3926–3933.
- [32] E. Peled, *J. Electrochim. Soc.* **1979**, *126*, 2047–2051.
- [33] J. Zhang, Z. Liu, Q. Kong, C. Zhang, S. Pang, L. Yue, X. Wang, J. Yao, G. Cui, *ACS Appl. Mater. Interfaces* **2012**, *5*, 128–134.
- [34] B. C. Yu, K. Park, J. H. Jang, J. B. Goodenough, *ACS Energy Lett.* **2016**, *1*, 633–637.
- [35] X. B. Cheng, T. Z. Hou, R. Zhang, H. J. Peng, C. Z. Zhao, J. Q. Huang, Q. Zhang, *Adv. Mater.* **2016**, *28*, 2888–2895.
- [36] R. Pathak, K. Chen, A. Gurung, K. M. Reza, B. Bahrami, J. Pokharel, A. Baniya, W. He, F. Wu, Y. Zhou, K. Xue, Q. Qiao, *Nat. Comm.* **2020**, *11*, 93–103.

Manuscript received: July 11, 2024
Revised manuscript received: September 11, 2024
Accepted manuscript online: September 20, 2024
Version of record online: October 30, 2024